3rd URSI AT-AP-RASC, Gran Canaria, 29 May – 3 June 2022

OTA 5G and Beyond Channel Evaluation in a Manufacturing Environment

Erik Kampert, Mahyar J. Koshkouei*, Yuen Kwan Mo, and Matthew D. Higgins
WMG, University of Warwick, Coventry, CV4 7AL, U.K.

Abstract

Low-latency, high-throughput wireless communication will strongly impact industrial automation systems, by enabling reconfigurable manufacturing, and remote process and quality control. The research presented here focuses on millimetre wave communication between elevated base stations and the manufacturing workshop area around a robotic optical scanner. The combination of fundamental channel sounding results and quality of signal parameters obtained from channel evaluation measurements highlights and explains the potential access to multigigabit wireless data throughput in such a challenging radio-frequency environment.

1 Introduction

Adaptive factories of the future are foreseen to rely on wireless instead of wired communication in order to establish versatile data transfer networks. Practically, a wireless communication system allows for full flexibility of factory resource usage; automatic adaptation, instant change of resource locations and optimisation of manufacturing processes without the need to re-wire communication links between components. This will go beyond the use of wheeled automated guided vehicles or quadruped agile mobile robots for goods transportation and process inspection, and is expected to require workshop machinery to transfer large data amounts to other tools or devices, which could be nearby or at a distance.

The focus of this study is therefore on understanding how millimetre wave (mmWave) communication in an industrial, manufacturing environment can be accurately described, how its quality can be estimated prior to and during transmission, and how it can be optimized for reliable, high-throughput, low-latency data exchange. Over-the-air (OTA) testing of the wireless communication performance in such environments is crucial to understand the impact of building materials, machinery/tools and potential interfering radio sources [1]. Ideally, a two-part approach is followed, combining the fundamental knowledge gained from channel sounding measurements with the Quality of Service (QoS) conclusions based on channel evaluation measurements [2]. The former yields accurate received power values for the investigated antenna constellations and the associated delay spread values that represent the environment's multipath richness, whereas the latter yields the error vector magnitude (EVM) and data throughput that are direct performance indicators for wireless communication applications.

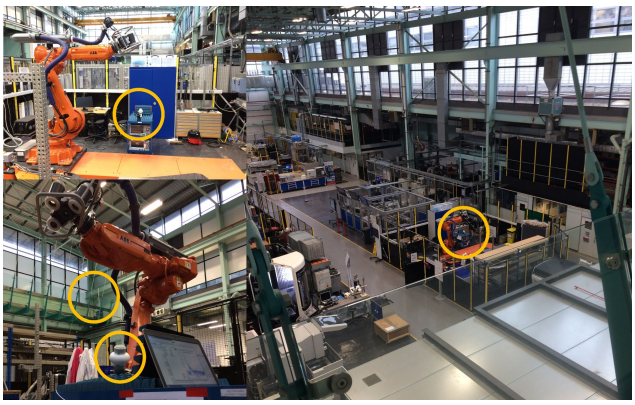

Figure 1. Channel sounding and evaluation near the 3D Optical Scanner with RX at position #7 (orange-encircled) and the TX boresight view from the left side of the bridge spanning the IMC Engineering Hall.

2 Experimental Details

Representing the prioritised first high frequency band for 5G in Europe and North America [3], for this particular study the focus is on the 3GPP band n257, thus using a carrier frequency (CF) of 28.5 GHz. As a specific future industrial communications application, a tool in a manufacturing chain requires high-definition images/videos from a 3D Optical Scanner (3D-OS) mounted on an industrial robot in WMG's International Manufacturing Centre's (IMC) Engineering Hall [4], shown in Figure 1, around which the presented channel sounding and evaluation measurements are carried out.

2.1 Channel Sounding

The WMG channel sounding equipment consists of an R&S SMW200A Vector Signal Generator, an R&S FSW85 Signal and Spectrum Analyzer and an R&S RTO2044 Digital Oscilloscope [5]. The former device enables the transmission of frequency band limited signals with CFs up to 40 GHz and arbitrary modulated waveforms with clock frequencies up to 2.4 GHz, and the latter two devices enable the process-

ing of the received signals with a maximum sampling rate of 2.4 GHz. The equipment is synchronized by means of direct, calibrated coaxial connections of their time reference and trigger channels. A 2 GHz bandwidth signal is generated and analysed, providing a time resolution of 0.5 ns, equivalent to a spatial resolution of 15 cm. For CFs up to 40 GHz, a filtered Frank-Zadoff-Chu sequence with a length of 120,000 samples is used as a channel sounding waveform, resulting in a channel impulse response update rate of 50 µs. Per antenna constellation 1024 CIR measurements are automatically triggered, and their results are stored, averaged and further analysed.

2.2 Channel Evaluation

The channel evaluation experiments, which provide both EVM and achievable data throughput measurements, are carried out using the NI mmWave Transceiver System (MTS) [5]. A multi-FPGA processing architecture enables to both capture and generate 2 GHz of data and to process it in real time. The MTS is built from a common set of hardware, with each PXIe-3610 DAC and PXIe-3630 ADC paired with a PXIe-3620 LO and IF module and a PXIe-7902 FPGA. A PXIe-6674T timing and synchronization module generates a trigger that is used to synchronize multiple channels and provides a higher quality 10 MHz clock source for better overall radio-frequency (RF) performance. External to the PXI chassis, the MTS is connected to a mmRH-3642 transmitter and a mmRH-3652 receiver mmWave radio head, optimised for the frequency band from 24.25 to 33.4 GHz, with 2 GHz instantaneous bandwidth and an analogue gain range of at least 50 dB. In addition to the RF hardware in the MTS, four additional FPGAs are added to the system to create a real-time 5G New Radio physical layer and to enable real-time encoding and decoding of the communication link's signal, which in turn enables a data throughput calculation. In its current state, the MTS software configuration follows the Verizon 5G specifications, using eight 100 MHz carriers resulting in a total 800 MHz bandwidth, a cyclic prefix orthogonal frequency-division multiplexing waveform, dynamic time-division duplexing, turbo coding, and quadrature phase shift keying, 16-QAM and 64-QAM as possible modulation schemes.

2.3 Antennas and cables

For both setups, the transmitter (TX) is a directional horn antenna with a typical gain of 23.6 dBi and a half-power beam width (HPBW) of 10° that focuses the RF signal into the direction of the receiver (RX), which in turn is an ultra-wideband omnidirectional antenna that is able to receive signals from any direction, with a typical gain of 6 dBi and a HPBW of 20° in its elevation plane. For the channel sounding, both the TX and RX are connected to their respective ends of the channel sounding equipment with 2 m long, low loss, phase-stable coaxial cables, which have a typical insertion loss of 4.8 dB each, plus 0.5 dB from a between-series coaxial adapter matching the input connector of the FSW85.

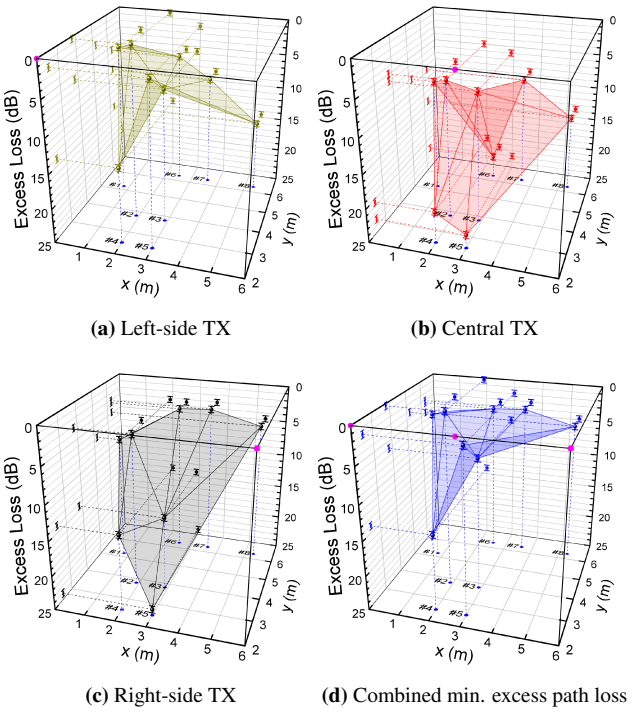

(a) Left-side TX **(b)** Central TX

(c) Right-side TX **(d)** Combined min. excess path loss

Figure 2. Excess path loss for various omnidirectional RX locations near the 3D-OS with TX positioned at (a) the left side, (b) the centre, and (c) the right side of a bridge spanning the workshop floor; and (d) the minimum excess path loss when combining the results from all three TX locations.

For each TX-RX antenna constellation, both antennas are manually bore-sight aligned with each other. Shorter, low loss, phase-stable coaxial cables are used for the channel evaluation measurements in order to obtain the highest possible RF TX output and RX input power, thereby establishing the largest possible range for a high-throughput communication link. These cables are 30 cm and 65 cm long and have a typical insertion loss of 1.0 dB, respectively 1.7 dB. Extensive component calibration prior to the measurements allows for a straightforward determination of the excess path loss, which cannot only be accounted for by free space path loss (FSPL).

3 Results and Discussion

Inside the safety mesh cage around the 3D-OS attached to the industrial robot, eight distinct omnidirectional RX locations are established on a floor area of 7x8 m. The local RF environments at these locations differ strongly, with clean line-of-sight (LoS) paths to the TX for some and obstructed (OLoS) or non-line-of-sight (NLoS) paths for others, e.g. due to vehicle door storage racks. The directional TX is subsequently placed at three elevated locations at ∼9 m above ground level, namely left, central and right on a bridge spanning the workshop floor. Figures 2a-c display the excess path loss at these selected locations for each TX-RX constellation, with Figure 2d combining the lowest excess path loss values of them, as could be achieved with three simultaneous

indoor base stations. The presented 3D-surfaces result from linear interpolation and interconnection of the measured values, supporting the prediction of the expected signal coverage of the 3D-OS working area. These excess path loss values are calculated based on the difference between the received power, the transmitted power, the transmitter and receiver antenna gains and losses, and the FSPL that in turn depends on the antenna separation, the carrier frequency, and the speed of light in vacuum. The use of FSPL, equal to a path loss exponent of 2, is supported by previously reported estimated large scale parameters in a production hall [6]. Any deviation from FSPL thereby highlights the investigated communication path being OLoS or NLoS.

It can be easily observed, that for all three TX locations the RX locations closer towards TX (smaller y) the excess path loss is higher, whereas for RX locations at a large distance the excess path loss can approach values close to 0 dB. The former directly demonstrates the effect of the vehicle door storage racks inside the 3D-OS area, which obstruct, block and reflect the LoS mmWave signal, with signal attenuation ranging from 5 dB to 25 dB. In general, each TX location results in a best signal propagation path to an RX closest to it, i.e. the left side of the investigated 3D-OS area (smaller x) is best covered by the left TX etc. Combining the lowest excess path loss results of all three TX locations then yields Figure 2d, which displays a good combined coverage for nearly all RX locations except for position #4.

Similarly the delay spread can be determined for each TX-RX constellation as presented in Figures 3a-c. The overall shapes of these 3D-surfaces resemble those in Figure 2, emphasising the inverse relation between received signal power and delay spread. This can be understood by the increased impact that multipath components have on a power delay profile with reduced or absent LoS signal, which weight in the delay spread is thereby reduced [7]. Moreover, the obstruction or blockage of the LoS signal path itself can also cause a strong reflection that then reaches RX over a longer communication path. Again, the combined minimum delay spread of TX placed at the left, centre and right elevated locations in Figure 3d results in small values except for position #4.

Finally, the QoS for a selection of antenna constellations is determined with channel evaluation measurements using a 64-QAM modulation scheme with a code rate of 7/8, by varying the MTS RF output power and recording the resulting EVM and data throughput values. TX is placed central on the bridge and RX is subsequently moved to all eight locations inside the 3D-OS safety cage. Only for four locations, namely #1, #2, #3 and #7, the signal quality is sufficiently high to enable a successful demodulation and decoding and result in a non-zero data throughput. The left plot in Figure 4 depicts how the data throughput performance for these four RX positions depends on the obtained EVM. Only below a threshold of ~ -25 dB can the full throughput of 2.8 Gb/s be obtained, corresponding with 3GPP Technical Specifications and previous reports [5, 7]. In the right plot of Figure 4 the received power spectral density (RPSD) dependence of the throughput is shown. The RPSD is obtained by dividing the received RX power by the selected MTS-bandwidth of 800 MHz, yielding a value that can be easily compared with other communication techniques. A minimum RPSD of -135 dBm/MHz is required to obtain a full throughput for a 64-QAM signal with a 7/8 code rate, which requirement is only fulfilled by RX-positions #2 and #3.

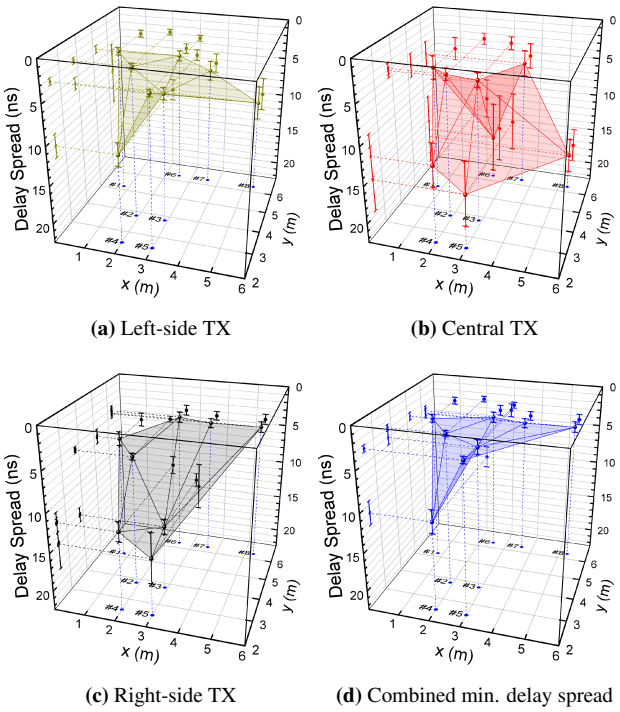

(a) Left-side TX **(b)** Central TX

(c) Right-side TX **(d)** Combined min. delay spread

Figure 3. Delay spread for various omnidirectional RX locations near the 3D-OS with TX positioned at (a) the left side, (b) the centre, and (c) the right side of a bridge spanning the workshop floor; and (d) the minimum delay spread when combining the results from all three TX positions.

4 Conclusions

The presented combination of mmWave channel sounding and evaluation results links the fundamental parameters of excess path loss and delay spread to the QoS parameters EVM and data throughput. For a high-throughput wireless connection to be established within the challenging RF environment of a manufacturing workshop, both the received power spectral density and the EVM need to beyond certain thresholds. The former is directly linked to the experienced path loss due to obstructions or blockages, whereas the latter can be associated to the signal-to-interference-plus-noise ratio due to multipath components, as interpreted in the signal's delay spread. For the investigated workshop area around a robotic optical scanner, these criteria are fulfilled for several TX-RX constellations, with others potentially benefiting from further research into smart antenna directivity and error correction optimisation.

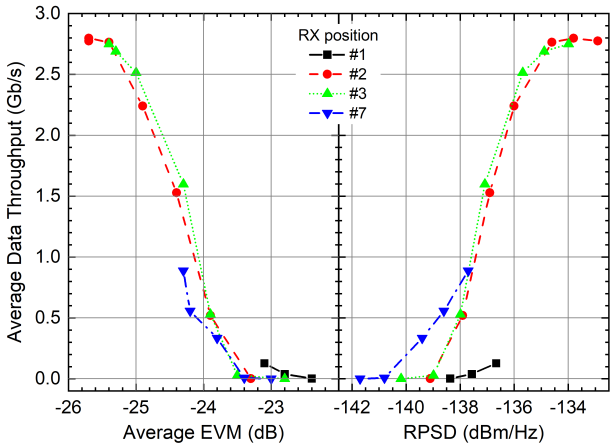

Figure 4. Measured averaged data throughput versus the EVM and RPSD between a 10° HPBW waveguide horn antenna and an ultra-wideband omnidirectional antenna at various RX locations in an industrial environment (see legend).

5 Acknowledgements

This work was supported in part by the WMG Centre High Value Manufacturing Catapult, University of Warwick, Coventry, U.K., and in part by the UK Engineering and Physical Sciences Research Council (EPSRC) through grant no. EP/N509796/1 and EP/R513374/1 and the EPSRC UK-RAS Network.

References

[1] T. H. Loh, D. Humphreys, D. Cheadle, and K. Buisman, "An Evaluation of Distortion and Interference Sources Originating Within a Millimeter-Wave MIMO Testbed for 5G Communications," in *2018 2nd URSI Atlantic Radio Science Meeting (AT-RASC)*, 2018, pp. 1–4.

[2] "5G QoS for Industrial Automation," 5G Alliance for Connected Industries and Automation (5G-ACIA), white paper, 2021, published by ZVEI e. V. [Online]. Available: https://5g-acia.org/wp-content/uploads/Whitepaper_5G-ACIA_5G-QoS-for-Industrial-Automation.pdf

[3] "Commission Implementing Decision (EU) 2020/590 of 24 April 2020 amending Decision (EU) 2019/784 as regards an update of relevant technical conditions applicable to the 24,25-27,5 GHz frequency band," *Official Journal of the European Union*, vol. L 138, pp. 19–22, 2020. [Online]. Available: https://eur-lex.europa.eu/legal-content/EN/TXT/PDF/?uri=CELEX:32020D0590&from=EN

[4] M. Babu, P. Franciosa, and D. Ceglarek, "Spatio-Temporal Adaptive Sampling for effective coverage measurement planning during quality inspection of free form surfaces using robotic 3D optical scanner," *Journal of Manufacturing Systems*, vol. 53, pp. 93–108, 2019. [Online]. Available: https://www.sciencedirect.com/science/article/pii/S0278612519300718

[5] T. H. Loh, Ed., *Metrology for 5G and Emerging Wireless Technologies*, ser. Telecommunications. Institution of Engineering and Technology, 2021, ch. 13 - Over-the-air testing for autonomous vehicle communications, pp. 413–447. [Online]. Available: https://digital-library.theiet.org/content/books/10.1049/pbte099e_ch13

[6] M. Schmieder, H. Klessig, A. Schultze, S. Wittig, M. Peter, and W. Keusgen, "Channel Measurements and Large Scale Parameter Estimation in a Production Hall," in *2021 IEEE 94th Vehicular Technology Conference (VTC2021-Fall)*, 2021, pp. 1–5.

[7] E. Kampert, C. Schettler, R. Woodman, P. A. Jennings, and M. D. Higgins, "Millimeter-Wave Communication for a Last-Mile Autonomous Transport Vehicle," *IEEE Access*, vol. 8, pp. 8386–8392, 2020.